

# Component structure of event-related fMRI responses in the different neurovascular compartments

Kenneth C. Roberts<sup>a</sup>, Tung T. Tran<sup>a,b</sup>, Allen W. Song<sup>c,d</sup>, Marty G. Woldorff<sup>a,e,\*</sup>

<sup>a</sup>Center for Cognitive Neuroscience, Duke University, Durham, NC 27708, USA

<sup>b</sup>School of Medicine, University of North Carolina–Chapel Hill, Chapel Hill, NC 27599, USA

<sup>c</sup>Brain Imaging and Analysis Center, Duke University Medical Center, Durham, NC 27708, USA

<sup>d</sup>Department of Radiology, Duke University Medical Center, Durham, NC 27708, USA

<sup>e</sup>Department of Psychiatry, Duke University Medical Center, Durham, NC 27708, USA

Received 17 January 2006; accepted 18 August 2006

## Abstract

In most functional magnetic resonance imaging (fMRI) studies, brain activity is localized by observing changes in the blood oxygenation level–dependent (BOLD) signal that are believed to arise from capillaries, venules and veins in and around the active neuronal population. However, the contribution from veins can be relatively far downstream from active neurons, thereby limiting the ability of BOLD imaging methods to precisely pinpoint neural generators. Hemodynamic measures based on apparent diffusion coefficients (ADCs) have recently been used to identify more upstream functional blood flow changes in the capillaries, arterioles and arteries. In particular, we recently showed that, due to the complementary vascular sensitivities of ADC and BOLD signals, the voxels conjointly activated by both measures may identify the capillary networks of the active neuronal areas.

In this study, we first used simultaneously acquired ADC and BOLD functional imaging signals to identify brain voxels activated by ADC only, by both ADC and BOLD and by BOLD only, thereby delineating voxels relatively dominated by the arterial, capillary, and draining venous neurovascular compartments, respectively. We then examined the event-related fMRI BOLD responses in each of these delineated neurovascular compartments, hypothesizing that their event-related responses would show different temporal componentries. In the regions activated by both the BOLD and ADC contrasts, but not in the BOLD-only areas, we observed an initial transient signal reduction (an *initial dip*), consistent with the local production of deoxyhemoglobin by the active neuronal population. In addition, the BOLD–ADC overlap areas and the BOLD-only areas showed a clear poststimulus undershoot, whereas the compartment activated by only ADC did not show this component. These results indicate that using ADC contrast in conjunction with BOLD imaging can help delineate the various neurovascular compartments, improve the localization of active neural populations, and provide insight into the physiological mechanisms underlying the hemodynamic signals.

© 2007 Elsevier Inc. All rights reserved.

**Keywords:** Functional MRI; BOLD; ADC; Event-related fMRI; Neurovascular; Hemodynamic

## 1. Introduction

For studies using functional magnetic resonance imaging (fMRI), the most commonly used indicator of neural activity is a transient increase in the blood oxygenation level–dependent (BOLD) signal, resulting mainly from an influx of new oxygenated blood into the region surround-

ing the active neural population. As cerebral blood flow (CBF) increases, the efficiency of oxygen extraction decreases, leading to a BOLD signal elevation that appears to originate mainly from capillaries, venules and larger draining veins [1,2]. Accurate localization of neural activity in functional imaging studies could be improved by contrasts that are more selectively sensitive to the part of the signal arising from the small vessels proximal to the site of the neural generators.

Isolating the capillary contribution of the BOLD signal has been a relatively elusive goal owing to the complexity of the hemodynamic response; factors such as the regional

\* Corresponding author. Center for Cognitive Neuroscience, Box 90999, Duke University, Durham, NC 27708, USA. Tel.: +1 919 681 0604; fax: +1 919 681 0815.

E-mail address: [woldorff@duke.edu](mailto:woldorff@duke.edu) (M.G. Woldorff).

volume of blood, the regional flow of blood and the concentration of deoxyhemoglobin in the blood all contribute differentially to the signal. Separating these changing individual contributions to the BOLD signal as the hemodynamic response unfolds in time is a difficult task and generally requires at least two separable physiological measures. Nonetheless, studies that investigated the physiologic changes underlying the BOLD signal have reached some consensus concerning some basic attributes of the response, although the finer points concerning the interaction of these factors remain controversial [3].

Perfusion imaging methods that measure CBF changes may provide better localization of the capillary hemodynamic response. However, many perfusion imaging methods rely on an injectable tracer, which makes this method less desirable for use in human populations. Other perfusion imaging methods that do not use injectable tracers rely on arterial spin labeling, in which a bolus of blood is “tagged” with an excitatory pulse and traced after several seconds to the locations in the brain that have increased CBF [4,5]. However, the temporal resolution is substantially lower than that in typical fMRI experiments using the BOLD contrast as the repetition rate for the stimuli has to be modified to allow for the transit time of the bolus. In addition, time must be allotted for the spin-labeled protons to diffuse into the parenchyma.

Intravoxel incoherent motion imaging uses diffusion-weighting methods to measure task-induced changes in blood flow that originate primarily in the arteries, arterioles and capillaries [6]. The apparent diffusion coefficients (ADCs) are calculated from a range of diffusion weightings that attenuate the ADC modulation for large vessels that have a slow and consistent flow. The observed task-induced changes in the ADC primarily come from smaller vessels having a faster and more turbulent flow: arteries, arterioles and capillaries. The method of calculating ADCs applied in the present report, developed in recent studies by Song et al. [7,8], uses a cyclical ramping of the diffusion weightings across sets of three consecutive time points and extracts the ADC by calculating an exponential fit to the signal across each of these time-point triplets. In addition, in this approach, the first time point of each three time points has a diffusion weighting of zero, thereby providing a conventional BOLD image for that time point. Acquiring the BOLD images simultaneously with the ADC signals in this way provides two (orthogonal) contrasts with the BOLD mainly sensitive to the capillary and venous compartments and the ADC mainly sensitive to the arterial and capillary compartments. Combining the information from these different signal contrasts allows for the delineation of these various neurovascular compartments, with the intersection of these contrasts (i.e., those regions activated by both contrasts) corresponding to the capillary regions closely associated with the neuronal activities [7,8].

During functional brain activity, the physiological events occurring within these neurovascular compartments are

bound to differ between the compartments and thus in turn contribute differentially to the signals recorded in functional imaging studies. In particular, the canonical event-related response of the widely used BOLD imaging approach has several components that have been used in functional mapping studies. The most robust and by far the most widely applied component of the BOLD signal is a large positive response (i.e., increase in BOLD signal) peaking 4–6 s after stimulus onset that arises from a large increase in CBF [2]. There is a strong consensus that this component is mostly venous/venule in origin, with also a capillary contribution [9,10]. Preceding this response in latency, a few studies have shown a small initial dip in the signal [9,11], which has been proposed to correspond to an initial increase in deoxyhemoglobin due to the extraction of oxygen by the metabolically active neural population [12]. This initial dip is relatively small and its ability to be robustly detected is still somewhat controversial, but its activation seems likely to be derived from the capillary network that is closer to the associated neural activity than the main BOLD positive peak and is more focal [12]. Following the main large positive peak of the BOLD response is a postpeak undershoot, a decrease in signal below baseline. Although the existence of this response component, which has been seen in numerous studies, is not doubted, its source and cause are not yet clear. It has been hypothesized by some researchers to be related to a slow effluxion of deoxyhemoglobin-rich blood from the venous compartment after the CBF has returned to baseline [13,14] but argued by others to be a result of sustained increases in oxygen utilization after the vascular response has recovered [15].

The present study describes event-related BOLD responses in regions of interest (ROIs) defined by the dual-contrast and enhanced spatial localization technique outlined above. That is, with the use of an initial set of block-design functional scanning runs in which both BOLD and ADC signals were simultaneously acquired, these ROIs were defined according to the relative level of activation by the ADC and BOLD contrasts so as to roughly correspond to the arterial, capillary and venous compartments. It should be noted that these voxels were not categorized as being composed exclusively of a given type of vasculature, given that we defined these ROIs on a voxelwise basis and each voxel was large enough to contain some vessels of all types. We instead identified each voxel according to what type of vessel likely dominated the observed signal coming from it.

After delineating these neurovascular compartments, we performed a second set of functional runs that were event-related in design. From these, we examined the differences in the BOLD event-related responses of these compartments. These analyses focused on whether any observed difference in the BOLD responses can be traced to predictions made from theoretical models of the underlying physiologic events and how they may differ depending on the neurovascular compartment in which the dominant response was recorded.

## 2. Methods

Fifteen subjects (mean age, 27 years; seven males) with no history of neurological disease were scanned in a General Electric SIGNA Lx 4-T whole-body MRI scanner at the Brain Imaging and Analysis Center of Duke University. All participants gave written informed consent to participate in the study. Five of the subjects were excluded from the final analyses because they exhibited excessive head motion or insufficient activation in either the ADC or BOLD contrasts, leaving 10 subjects who were included in the final analysis.

### 2.1. Stimuli

Subjects wore LCD goggles during scanning and were instructed to fixate on a small cross at the center of their field of view. Corrective lenses were used for all subjects who needed them, and a closed-circuit camera was used to monitor subjects' eye movements. The stimuli were a pair of checkerboards formed from a 6×8 grid of squares (vertical × horizontal). These were positioned in the lower left and right visual fields, centered 2.5° inferior and 4° lateral of the fixation, approximating the location used in several of our previous experiments in visual perception and spatial attention [16–18] (Fig. 1). Each check square subtended 0.5° of visual angle and flickered at 10 Hz (i.e., on for 100 ms and off for 100 ms), approximately an optimal size and frequency for producing vigorous hemodynamic activation in the visual cortex [19].

### 2.2. Localization of ADC and BOLD compartments

For the first set of functional scans, six oblique axial slices were chosen such that the imaging plane was parallel to and centered on the calcarine sulcus, covering areas of the primary visual cortex corresponding to the location of the

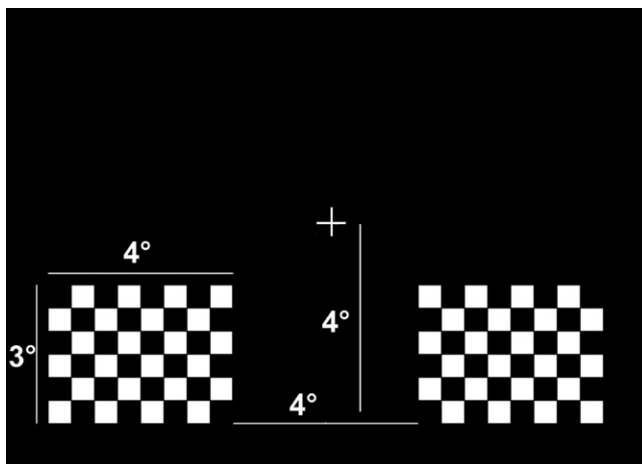


Fig. 1. Visual stimulus used for all experiments, shown with a fixation cross. Four additional notation lines are included in the figure to indicate dimensions. These bilateral checkerboard stimuli were flickered at 10 Hz (inverted every 100 ms) for 500 ms in the lower hemifield, which is represented in the portion of the primary visual cortex lying on the superior bank of the calcarine fissure.

stimuli in the visual field (isotropic 3.75-mm voxels; echo time=50 ms; flip angle=60°). In these runs, a block-design paradigm with simultaneously acquired ADC and BOLD contrasts was used to localize the neurovascular compartments responding to the bilateral lower-visual field flickering checkerboard stimuli. This set consisted of six runs, each of 210-s duration and containing alternating 30-s “off” and “on” cycles, beginning with an “off” cycle and with stimuli presented only during the three “on” cycles. The repetition time (TR) for these combination ADC–BOLD runs was 1 s. High-resolution  $T_1$ -weighted spin-echo structural images were also acquired to provide an anatomical reference for the functional activity.

In the block functional scans described above, the diffusion-weighting  $b$ -factor was cycled through the values of 0, 114 and 229 s/mm<sup>2</sup> during each successive three TRs to derive the ADC values. Isotropic weighting gradients were embedded into a gradient-recalled spiral imaging sequence, as described in an earlier study [7]. For each 3-s cycle of the functional run, an ADC value was determined using a simple exponential fit based on the relationship that

$$F = e^{-bD}$$

where  $F$  is the signal attenuation factor due to diffusion,  $b$  is the diffusion-weighting factor and  $D$  is the ADC. An exponential fitting routine was carried out for each cycle of dynamic diffusion weighting, thereby yielding a dynamic time course of ADC values. For each subject, the dynamic ADC time courses were fit with a spline function and averaged together across runs to improve statistical significance.

Because of the dynamic cycling of the diffusion-weighting  $b$ -factor values, the  $b$ -factor was equal to zero at every third time point (i.e., every third TR) during the image acquisition. Thus, an extraction of these samples yielded a sequence across time of conventional BOLD functional images acquired simultaneously with the ADC-derived images.

For each subject, voxels were chosen separately from the BOLD functional time course and the ADC functional time course if they showed an increase in activation during the “on” cycle, with a significance of  $t > 4.00$ . Voxels activated by the ADC but not the BOLD time formed an ADC-only ROI for each subject, those activated by the BOLD but not the ADC formed a BOLD-only ROI and those that were jointly active for both signal measures formed an ADC–BOLD overlap ROI.

### 2.3. Event-related BOLD responses

In the second set of functional imaging runs, an event-related visual stimulation paradigm was used to estimate the impulse response function of the BOLD signal in each of the ROIs associated with the various neurovascular compartments as described above. The same six slices were imaged without diffusion weighting. Four of these event-related runs were recorded for each subject, consisting of 20 trials of 15-s

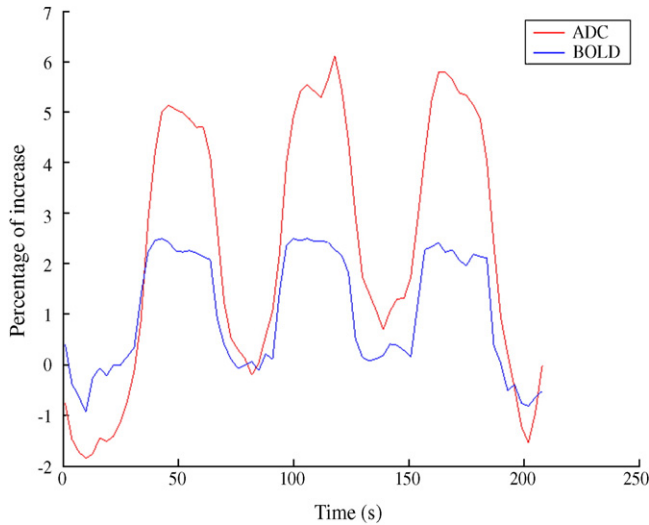


Fig. 2. Signal time courses in the block-design paradigm grand averaged across subjects. Plots of the ADC signal change observed in areas activated by the ADC contrast and the BOLD signal change observed in areas activated by the BOLD contrast are shown.

duration each, with the visual stimulus checkerboard flickering during the first 500 ms of each trial. A long interstimulus interval was used to minimize hemodynamic response function overlap. A TR of 500 ms was used to better sample the temporal characteristics of the event-related hemodynamic responses. With a 500-ms TR and allowing 5 s at the beginning of each run for the signal to stabilize, 610 volume images were acquired for each 305-s run of 20 trials.

For each subject, the hemodynamic response function was calculated by averaging each epoch time locked to the

onset of the stimulus across each of the ADC-only, BOLD-only and ADC–BOLD overlap ROIs. These responses were averaged and analyzed over subjects to provide population estimates of the BOLD response in each compartment and were then converted into units of percentage of signal change from baseline using a prestimulus baseline epoch of  $-1.5-0$  s. Periods of the averaged BOLD responses that corresponded to the components of interest in the hemodynamic response were analyzed. The initial dip epoch was evaluated for the interval ranging from 0 to 1.5 s, the main positive response was evaluated from 4 to 5.5 s and the undershoot was evaluated from 8.5 to 13.5 s. For the comparison of these response components between compartments, the percentage of signal change was averaged over the epoch of interest and compared using a paired  $t$  test across subjects.

### 3. Results

#### 3.1. Localization of the neurovascular compartments

Both the ADC and BOLD contrasts showed robust activations during the neurovascular compartment localization runs, as evidenced by the grand-averaged time courses. ADC activation showed synchronized and robust activation during the task period, with magnitudes of both percentage changes and variances larger than those with BOLD activation (Fig. 2).

The neurovascular compartments were derived from the areas activated during the block-design visual stimulation runs using both the ADC and BOLD contrasts. As discussed in the Methods section, three regions were characterized: the

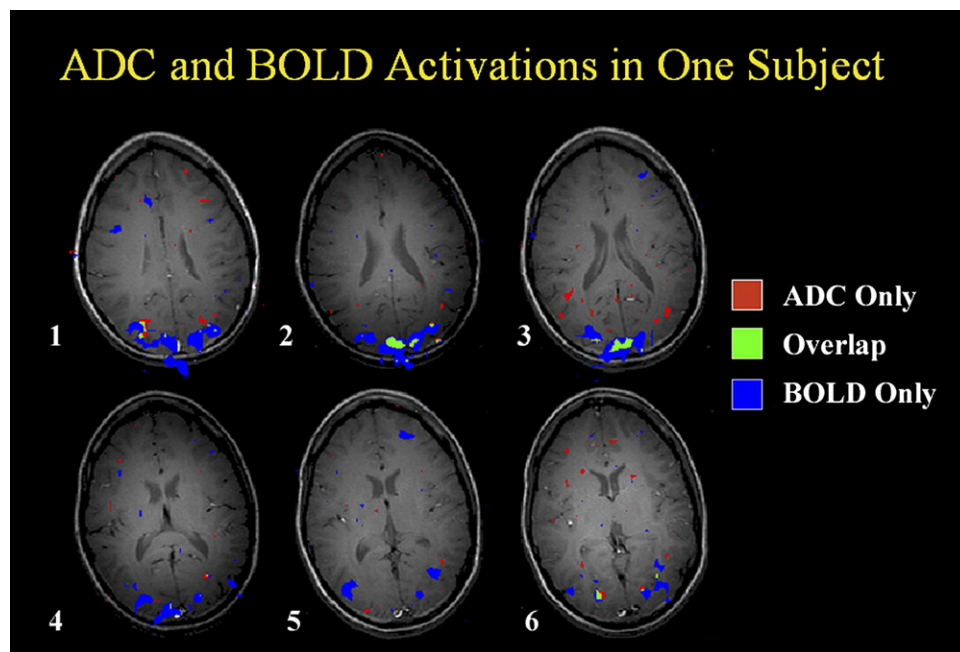


Fig. 3. An example of the three neurovascular compartment ROIs derived from the BOLD and ADC signals in a single subject. The slices are numbered from superior to inferior and chosen such that the calcarine fissure lay between the third and fourth slices. Notice that the overlap of the two compartments is symmetric about the medial fissure and for the most part confined to the superior bank of the calcarine fissure (slices 1–3).

ADC-only, ADC–BOLD overlap and BOLD-only regions. In single subjects, at the same level of statistical significance, the BOLD activation consistently encompassed a larger area than did the ADC activation (Fig. 3). Both the ADC and BOLD activations were observed bilaterally on the superior bank of the calcarine sulcus (Figs. 3 and 4), which is consistent with the known retinotopy of the primary visual cortex (V1) for visual stimuli in the lower visual field [20–22]. However, there was considerable residual BOLD activation also seen on the lower bank of the calcarine sulcus, presumably due to some portion of the signal arising from veins that drain the upper bank of the sulcus, thus reflecting some of the limitations of the precision of BOLD-based neuronal localization. The overlapping region between the ADC and BOLD activated areas, which should presumably be dominated by the capillary regions proximal to the actual neuronal activity, showed robust activation restricted to the superior bank of the calcarine and away from the occipital pole, corresponding appropriately to the peripheral lower-field visual stimulation that was used.

### 3.2. Event-related responses in the neurovascular compartments

BOLD time courses from the event-related visual stimulation runs were extracted and averaged within these compartments to more closely assess the signal origins and response componentries of the aforementioned three compartments identified by the ADC and BOLD activations. The grand-averaged event-related time courses across subjects for the three ROI compartments, given in units of percentage of signal change, are plotted in Fig. 5.

As expected, the ADC–BOLD overlap and BOLD-only regions showed large amplitudes of the main positive BOLD signal change, with the ADC-only region showing a much smaller response as compared with the other two compartments. This was reflected statistically by there being a significantly larger BOLD signal amplitude over the time interval (4–5.5 s) corresponding to the positive response (two-tailed *t* test of the ADC-only region against the ADC–

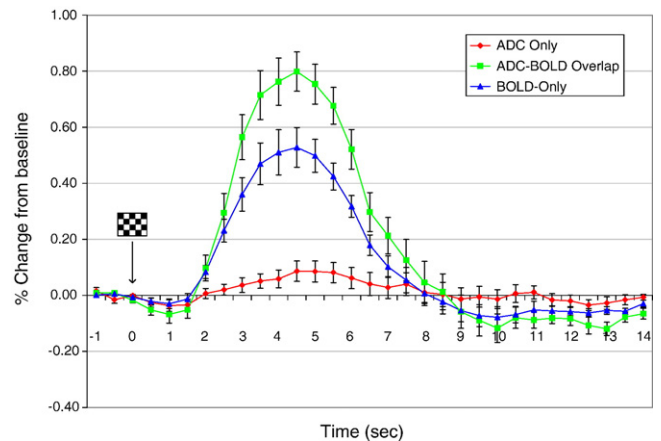


Fig. 5. The event-related BOLD response in each of the three neurovascular compartments grand averaged across the 10 subjects. Note that each time point represents the signal from the half-second interval immediately prior to that time point.

BOLD region and the ADC-only region against the BOLD-only region; each significant at  $P < 10^{-5}$ ). In addition, this main BOLD response was larger in the ADC–BOLD overlap region than in the BOLD-only region (two-tailed *t* test;  $P = .001$ ).

Immediately after the onset of the stimuli, the ADC–BOLD overlap region showed a small but significant transient signal reduction (one-tailed *t* test against a prestimulus baseline;  $P = .013$ ). This observation supports the existence of an initial dip in the capillary networks. Interestingly, the ADC-only region also showed a smaller but also significant initial dip that could be due to the inclusion of the small arterioles where oxygenation extraction would occur ( $P = .05$ ). The initial dip was not significant in the BOLD-only region.

After the main positive BOLD response, the ADC–BOLD overlap and BOLD-only regions showed a large signal undershoot (two-tailed *t* test against baseline yielded  $P = .009$  and  $P = .017$  for the ADC–BOLD overlap region and the BOLD-only region, respectively). In contrast, the

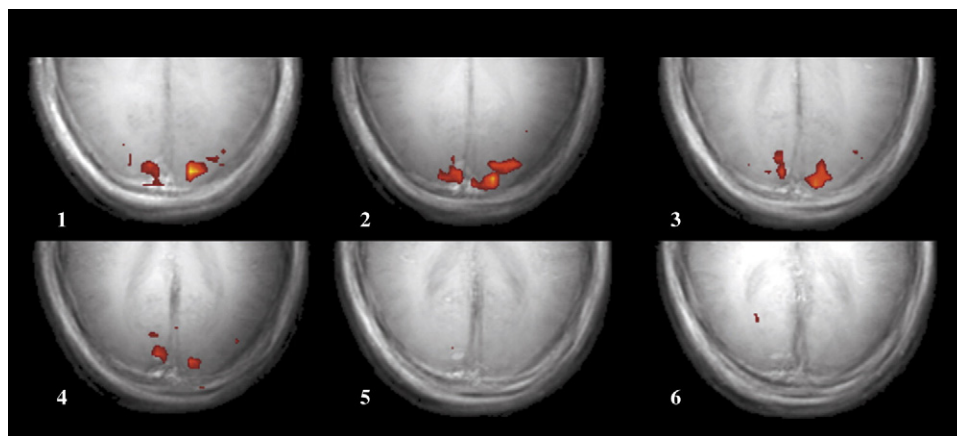


Fig. 4. Map of the areas activated by the ADC contrast. This figure was derived from a random effects analysis of the ADC activation across subjects. The collapsing across subjects for this figure was performed after rigidly aligning (i.e., anchoring) the individual subject contrasts with respect to the occipital pole.

ADC-only region did not exhibit a poststimulus undershoot ( $P > .6$ ).

#### 4. Discussion

In this study, we first performed a series of block-design functional imaging runs using an MR pulse sequence that allowed the simultaneous extraction of both ADC and BOLD signals, the combination of which then allowed the delineation of voxels relatively dominated by the different vascular compartments. This was followed by a conventional event-related BOLD contrast paradigm using selective averaging and the extraction of the three hemodynamic response functions for the venous-dominated, capillary dominated and arterial-dominated compartments as delineated by the ADC–BOLD analyses. The response waveforms for these three compartments were unique with respect to the salient features of the canonical hemodynamic response: the initial dip, the main positive response and the poststimulus undershoot. These differences may be understood in the context of the prevailing theories of the physiologic bases of the contribution of each vascular compartment to these features of the hemodynamic response.

The possibility that the BOLD signal would show an initial dip was first hypothesized with the use of optical imaging by Grinvald et al. [23], who observed a brief local increase in deoxyhemoglobin optical signal in the active cortex preceding a large rise in the oxyhemoglobin signal (caused by the increased CBF corresponding to the positive BOLD response). These two effects, which can be independently observed by optical measurement recording signals at different wavelengths, become conflated when measured with the BOLD contrast. Several researchers [9,11] reported observing this initial dip in fMRI experiments in certain voxels and attributed it to the contribution of signal from the capillary bed close to the true neuronal activity. Kim et al. [24] took advantage of the increased spatial specificity of the initial dip to report on the mapping of ocular dominance columns in cat visual cortices. These fMRI studies functionally identified voxels depending on whether they showed a significant initial dip in the BOLD signal and used the optical imaging studies to provide a theoretical frame for the argument that the voxels were corresponding to the capillary compartment. The present study helps strengthen the connection between these two previous lines of work by providing a means of identifying the capillary compartment that uses an independent measure from the BOLD signal, is based on the physiology of the blood flow and turbulence characteristics of the capillary compartment, and can be incorporated into existing fMRI designs.

In the present study, we observed a significant initial dip in the event-related responses in the ADC–BOLD overlap compartments and a smaller, marginally significant one in the ADC-only compartment. In contrast, the time course

averaged over the BOLD-only region did not show a significant initial dip, consistent with it being derived mainly from large venules and veins. In these regions, by the time the blood with an increased concentration of deoxyhemoglobin starts to reach and collect in the venous compartment, its influence would be overwhelmed by the influx of oxygenated blood that gives rise to the positive BOLD response. Accordingly, the initial dip, arising from an accumulation of deoxyhemoglobin, would be counteracted by the beginning of the positive response of the BOLD signal. Only in areas exhibiting a particularly strong and focal increase in deoxyhemoglobin would the signal dip transiently override the positive signal increase due to the oxygenated blood influx and cause an overall transient dip in the signal.

As expected, the main positive response was much stronger in the ADC–BOLD overlap and BOLD-only regions than in the ADC-only region. In that the ADC-dominated voxels would be expected to most closely correspond to the arteriole and artery neurovascular compartments, which would be mostly located upstream of the active neural population and active oxygen extraction, the blood at that point should be highly oxygenated. Accordingly, these regions would not be expected to show significant event-related BOLD signal changes. Another observation in the present data was that, although the ADC–BOLD overlap and BOLD-only regions both showed strong levels of the main positive response after spatial averaging, the response in the ADC–BOLD overlap region was significantly larger than that of the BOLD-only one. This result suggests that the focal capillary dominated regions may be able to contribute a fairly concentrated main BOLD response and that the venous contribution, although substantial, is more broadly distributed across a much higher number of voxels, as demonstrated by its larger spatial extent.

Lastly, a poststimulus undershoot was observed in the ADC–BOLD overlap and BOLD-only regions. The undershoot may be due to a vessel dilation [14] or an elevated metabolic state persisting after brain activation [15]. In either case, the origin of the undershoot is predicted to be localized primarily to the venous compartment; thus, its presence in the present study helps confirm the hypothesized origin of the functional signal coming from this compartment. In contrast, the ADC-only region did not show a significant poststimulus undershoot. This observation is consistent with the reported characteristics of the CBF changes as blood flow would quickly return to baseline at the offset of brain activation.

#### 5. Conclusions

The differing componentries of the responses provide support for several current theories concerning the physiology of the BOLD response in the various vessel types while also helping confirm that the different neurovascular

compartments can be functionally separated using our ADC–BOLD technique. The active neural population regions appear to be appropriately associated with the compartment identified by the ADC–BOLD overlap, with its localization being considerably more precise than that which would be obtained with the BOLD contrast alone.

### Acknowledgments

This work was supported by grants from the NIMH (R01 MH 60415) and the NINDS (P01 NS 41328; Project 2) to M.G.W. as well as those from the NSF (BES 0092672) and the NINDS (R01 NS 50329) to A.W.S.

### References

- [1] Kwong KK, Belliveau JW, Chesler DA, Goldberg IE, Weisskoff RM, Poncelet BP, et al. Dynamic magnetic resonance imaging of human brain activity during primary sensory stimulation. *Proc Natl Acad Sci U S A* 1992;89:5675–9.
- [2] Ogawa S, Menon RS, Tank DW, Ugurbil K. Functional brain mapping by blood oxygenation level dependent contrast magnetic resonance imaging. *Biophys J* 1993;29:277–9.
- [3] Buxton RB. Commentary: the elusive initial dip. *Neuroimage* 2001; 13:953–8.
- [4] Detre JA, Leigh JS, Williams DS, Koretsky AP. Perfusion imaging. *Magn Reson Med* 1992;39:855–64.
- [5] Ye FQ, Pekar JJ, Jezzard P, Duyn J, Frank JA, McLaughlin AC. Perfusion imaging of the human brain at 1.5 T using a single shot EPI spin tagging approach. *Magn Reson Med* 1996;36:217–24.
- [6] Turner R, Le Bihan D, Maier J, Vavrek R, Hedges LK, Pekar J. Echo planar imaging of intravoxel incoherent motion. *Radiology* 1990; 177:407–14.
- [7] Song AW, Fichtenholz HM, Woldorff MG. BOLD signal compartmentalization based on the apparent diffusion coefficient. *Magn Reson Imaging* 2002;20:21–525.
- [8] Song AW, Woldorff MG, Gangstead S, Mangun GR, McCarthy G. Enhanced spatial localization of neuronal activation using simultaneous apparent-diffusion-coefficient and blood-oxygenation functional magnetic resonance imaging. *Neuroimage* 2002;17:742–50.
- [9] Menon RS, Ogawa S, Strupp JP, Ugurbil K. Ocular dominance in human V1 demonstrated by functional magnetic resonance imaging. *J Neurophysiol* 1997;77:780–7.
- [10] Song AW, Wong EC, Tan SG, Hyde JS. Diffusion weighted fMRI at 1.5 T. *Magn Reson Med* 1996;34:155–8.
- [11] Hu X, Le TH, Ugurbil K. Evaluation of the early response in fMRI in individual subjects using short stimulus duration. *Magn Reson Med* 1997;37:877–84.
- [12] Malonek D, Grinvald A. Interactions between electrical activity and cortical microcirculation revealed by imaging spectroscopy: implications for functional brain mapping. *Science* 1996;272:551–4.
- [13] Frahm J, Kruger G, Merboldt K, Kleinschmidt A. Dynamic uncoupling and recoupling of perfusion and oxidative metabolism during focal brain activation in man. *Magn Reson Med* 1996; 35:143–8.
- [14] Buxton RB, Wong EC, Frank LR. Dynamics of blood flow and oxygenation changes during brain activation: the balloon model. *Magn Reson Med* 1998;39:855–64.
- [15] Lu H, Golay X, Pekar JJ, Van Zijl PC. Sustained poststimulus elevation in cerebral oxygen utilization after vascular recovery. *J Cereb Blood Flow Metab* 2004;24:764–70.
- [16] Woldorff MG, Fox PT, Matzke M, Lancaster JL, Veeraswamy S, Zamarripa F, et al. Retinotopic organization of early visual spatial attention effects as revealed by PET and ERPs. *Hum Brain Mapp* 1997;5:280–6.
- [17] Woldorff MG, Liotti M, Seabolt M, Busse L, Lancaster JL, Fox PT. The temporal dynamics of the effects in occipital cortex of visual–spatial selective attention. *Brain Res Cogn Brain Res* 2002;15:1–15.
- [18] Woldorff MG, Hazlett CJ, Fichtenholtz HM, Weissman DH, Dale AM, Song AW. Functional parcellation of attentional control regions of the brain. *J Cogn Neurosci* 2004;16(1):149–65.
- [19] Miki A, Liu GT, Goldsmith ZG, Zhou L, Siegfried J, Hulvershorn J, et al. Effects of check size on visual cortex activation studied by functional magnetic resonance imaging. *Ophthalmic Res* 2001; 33:180–4.
- [20] Jeffreys DA, Axford JG. Source locations of pattern specific components of human visual evoked potentials: I. Components of striate cortical origin. *Exp Brain Res* 1972;16:1–2.
- [21] Jeffreys DA, Axford JG. Source locations of pattern specific components of human visual evoked potentials: II. Components of striate cortical origin. *Exp Brain Res* 1972;16:22–40.
- [22] Sereno MI, Dale AM, Reppas JB, Kwong KK, Belliveau JW, Brady TJ, et al. Borders of multiple visual areas in humans revealed by functional magnetic resonance imaging. *Science* 1995;268:889–93.
- [23] Grinvald A, Frostig RD, Siegel RM, Bartfeld E. High resolution optical imaging of functional brain architecture in the awake monkey. *Proc Natl Acad Sci U S A* 1991;88:11559–63.
- [24] Kim DS, Duong TQ, Kim SG. High-resolution mapping of iso-orientation columns by fMRI. *Hum Brain Mapp* 2000;3:164–9.